# Simplified Reactive Power Control of a Multilevel Inverter for Grid-Connected Photovoltaic Applications

1st Francisco Perez-Cuapio
*TecNM-Instituto Tecnológico de Apizaco*
*Div.de Estudios de Posgrado e Investigación*
Av. Instituto Tecnológico s/n, Apizaco, Tlaxcala, México
E-mail: jfranciscoperezc7@gmail.com

2nd Roberto Morales-Caporal
*TecNM-Instituto Tecnológico de Apizaco*
*Div. de Estudios de Posgrado e Investigación*
Av. Instituto Tecnológico s/n, Apizaco,Tlaxcala, México
E-mail: rmcaporal@hotmail.com

3rd Marco A. Morales-Caporal
Universidad Politecnica de Tlaxcala
Av. U. Politecnica, No.1, Xalcaltzinco, Tlaxcala, México
E-mail: marcoantonio.morales@uptlax.edu.com

***Abstract*— Photovoltaic generation has grown with continuous developments that allow new functionalities such as power factor correction or multilevel voltage generation. However, the increment in the complexity of control algorithms requires expensive digital systems for their correct implementation. Therefore, this paper presents a new simplified reactive power control technique based on the d-q rotating frame theory allowing power factor correction by injecting phase-shifted or in-phase current to the power grid from photovoltaic arrays. Furthermore, the high conversion efficiency rate result is due to the use of an MPPT algorithm. Finally, the proposed simplified reactive power control was constructed to be used in a 7-level H-bridge power inverter. Simulated results of the proposed simplified control scheme verify low-THD in the current and a high-performance during active or reactive power injection into the single-phase electrical grid.**

***Keywords—photovoltaic array, current control, grid-connected, multilevel inverter, single-phase control, reactive power control.***

## I. INTRODUCTION

In the development of solar generation systems, there has been a trend towards integrating a more significant number of capacities with a pursuit to lower the number of electronic devices [1]. Through multilevel topology, some advantages such as current with low harmonic distortion, the increase in the power capability of the inverter, and small size of the output filters can be reached due to the type of step voltage the system generates[2].

However, this type of inverter has the disadvantage of requiring a complex control system due to multilevel modulation algorithms and the necessity of software sections to operate added systems. Some added systems can be; reactive power injection, which allows an improvement on the quality of electrical power at the Common Connection Point (CCP), [3], [4] or the balancing of the power generated by the different arrays of solar panels, to operate with partial shading conditions [2]. These drawbacks result in more software sections inside the control to perform all the functions successfully.

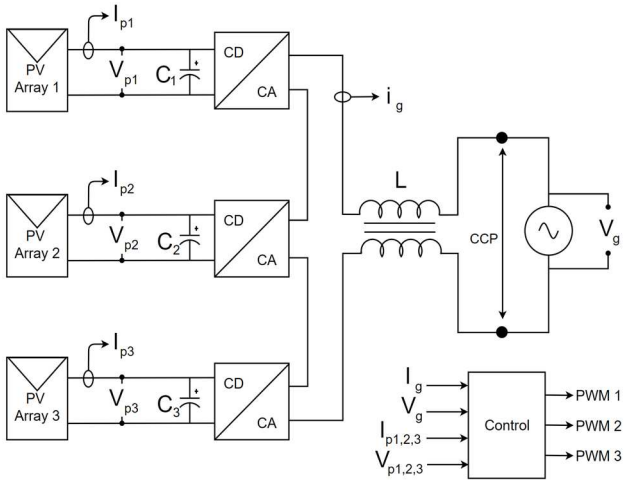


Fig. 1. Simplified diagram of the single-phase 7-level inverter based on three cascaded H-bridges.

Another problem related to the complexity of the control algorithm is the need for a powerful and expensive digital system required to execute the entire algorithm every switching period, resulting in the use of expensive technologies like FPGAs [5].

To solve this problem, a new control system is proposed to operate a 7-level inverter with active and reactive power injection capability through a low-complexity control algorithm that allows using a cascaded H-bridge multilevel topology as power hardware.

## II. STUDIED SYSTEM

In this research, a 7-level inverter was built with three cascaded H-bridges using IGBT transistors as power switches. Each H-bridge is fed by an array of two solar panels connected in series, generating a total of 61.92 Volts at the maximum power point. A 2400 µF capacitor is used to stabilize the array voltage, and a 2.2 mH common-mode inductive filter is added between the output of the multilevel inverter and the single-phase distribution grid modeled as an AC voltage source. In total, 6

978-1-6654-0029-9/21/$31.00 ©2021 IEEE

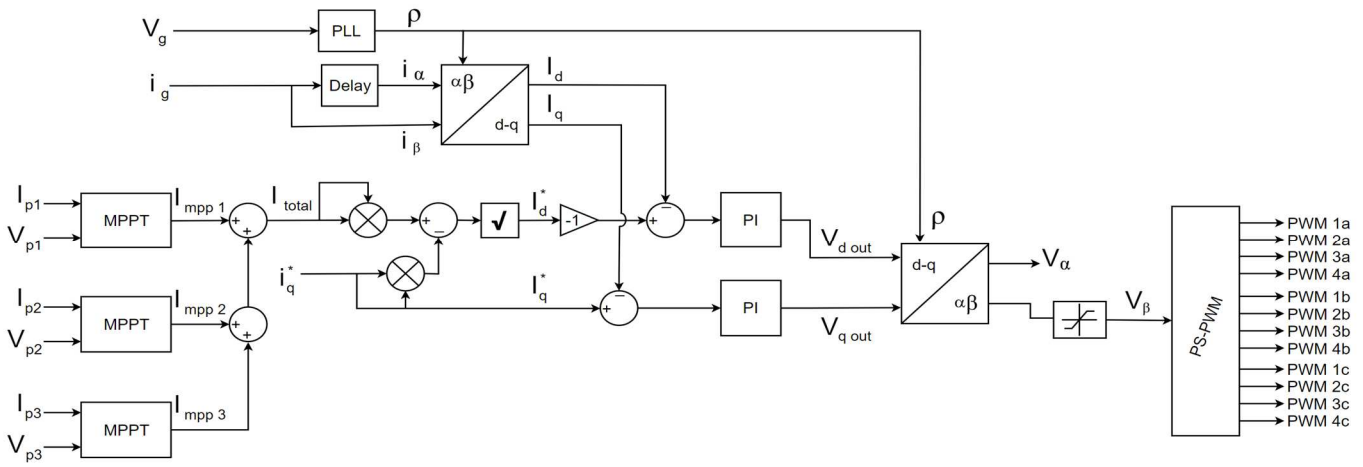


Fig. 2. Proposed control scheme

Solartec solar panels model S60MC-250 are used, and each one delivers 250 Watts of power at its maximum generation point [6]. A schematic of the 7-level inverter used in this research can be seen in Fig. 1.

This inverter follows the single-stage structure replacing with a capacitor the DC-DC converter used in the double-stage topologies [7]–[9]. This reduction in the number of circuits allows lower hardware costs and increases the inverter's efficiency since fewer switching elements dissipate power.

A common-mode L-type filter is used to reduce current harmonic distortion (THD) at the output. These filters are simpler than LCL filters used in [10] and have a smaller size than their single-coil counterparts; moreover, common-mode filters can tolerate higher currents and have lower magnetic saturation in the core due to the arrangement coils [11].

On DC stage, voltage and current sensors are placed at the output of each of the three solar panel arrays to calculate the maximum power point [12], [13]. On the other hand, the AC stage sensors are placed in two different sections at the output of the multilevel inverter. The voltage sensor is placed at the terminals of the single-phase AC distribution network after the inductive filter, while the current sensor is placed before the filter. With the voltage sensor and the PLL block, the angle ρ of the single-phase voltage signal can be estimated, while with the current sensor, the feedback information for inverter control is obtained.

The measurement of feedback current is taken before the inductive filter. If a load was connected at the common connection point (CCP), the current demanded by the load could affect the control feedback loop. Therefore, only by placing the sensor before the inductive filter, the output current of the multilevel inverter is measured, and this change gives the system the ability to inject current into the grid or assist the single-phase grid in the generation of electric power for the consumption of a load connected at the CCP.

## III. CONTROL ALGORITHM PROPOSAL

The proposed algorithm presented in this work is shown in Fig. 2. Due to the low conversion rate of the solar panels, it is necessary to extract the maximum power from each of the arrays to increase the efficiency of the developed system [2], [14]. For this purpose, the maximum current of every photovoltaic array $I_{pmm1,2,3}$ is calculated through the Maximum Power Point Tracking algorithm (MPPT) known as Incremental Conductance (IncCond). The IncCond algorithm is used to calculate the current at the maximum power point using voltage and current sensors placed at the output of the solar panels. The calculation of the currents $I_{pmm1,2,3}$ is performed as shown in the flowchart in Fig. 3.

When the maximum power current of each of the PV arrays ($I_{mpp\ 1,2,3}$) is estimated, these values are summed as seen in (1) to obtain the total maximum power current $I_{total}$, which is used to estimate the current references the PI controllers.

$$I_{total} = I_{mpp1} + I_{mpp2} + I_{mpp3} \quad (1)$$

This control proposal assumes equal and uniform solar radiation on all solar panels; therefore, the stage responsible for balancing the currents drawn from each PV array is omitted. It is possible to maintain the simplicity of the control algorithm.

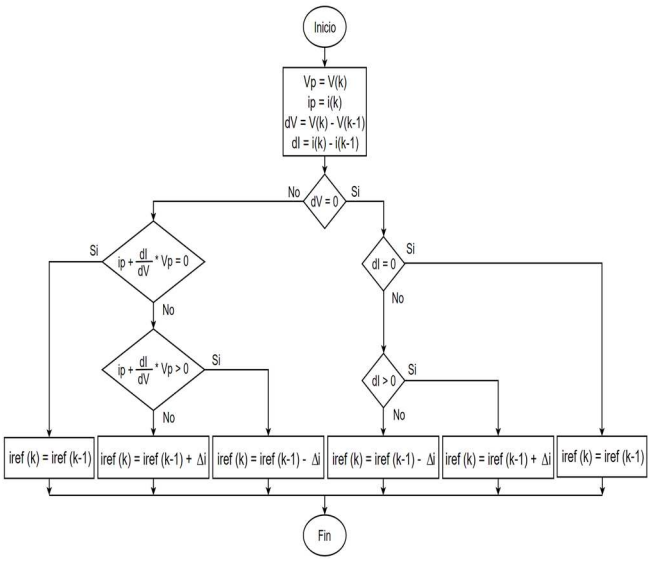


Fig. 3. Flowchart of the MPPT algorithm used for the calculation of the reference current.

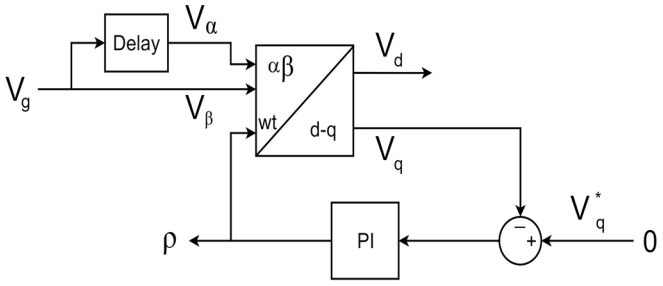


Fig.4. PLL block diagram

By measuring the grid voltage and using a single-phase PLL, the value of the angle $\rho$ of the grid voltage is estimated. The structure of the PLL used can be seen in Fig. 4. Through cascaded low pass filters, two current signals, $i_\alpha$ and $i_\beta$ shifted 90° from each other, are generated from the output current $i_g$ of the multilevel inverter. With the current signals $i_\alpha$ and $i_\beta$ together with the voltage angle $\rho$, Park's transformation is performed to obtain $I_d$ and $I_q$ in the rotating reference frame d-q. These currents are used as feedback values in the PI controls. To generate $I_d^*$ and $I_q^*$ from $I_{total}$, $I_q^*$ is assigned a value equal to or less than $I_{total}$, and the calculation of the reference component $I_d^*$ is performed by (2).

$$I_d^* = \sqrt{{I_{total}}^2 - {I_q^*}^2} \tag{2}$$

The reference currents $I_d^*$ and $I_q^*$ are used to calculate the PI controls' error values through (3) and (4). To estimate the error of the PI control of the d component, $I_d^*$ must change the sign. In the computation of $I_q^*$, there is no change.

$$I_{d_{error}} = (-1) * I_d^* - I_d \tag{3}$$

$$I_{q_{error}} = I_q^* - I_q \tag{4}$$

Table I shows the values of the PI controls used in this control proposal.

TABLE I PI CONTROLLER PARAMETERS

| | |
|---|---|
| **Controller of the d component** | |
| ***Proportional*** | 0.09 |
| ***Integral*** | 2.95 |
| **Controller of the q component** | |
| ***Proportional*** | 0.087 |
| ***Integral*** | 4.8 |
| **PLL** | |
| ***Proportional*** | 0.0034 |
| ***Integral*** | 21 |

The results obtained at the output of the two PI controls are the voltage components $V_{d_{out}}$ and $V_{q_{out}}$, which are in the d-q frame. An inverse Park transformation is performed to obtain the control signal, and two sine signals $V_\alpha$ and $V_\beta$, are obtained. Since the developed system is single-phase, only the $V_\beta$ component is used as the control signal.

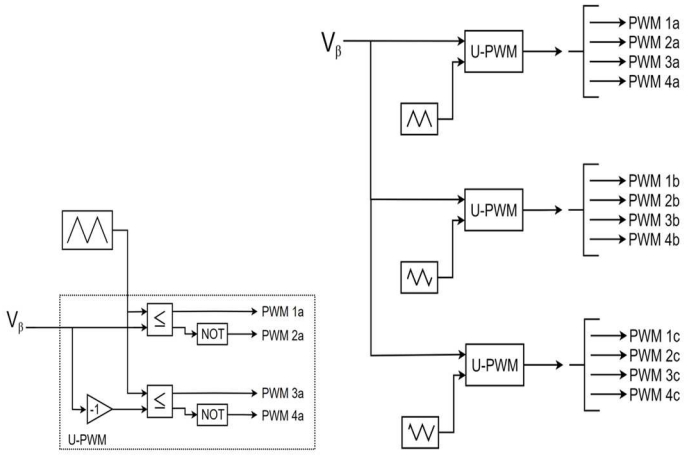


Fig.5. Scheme of the 7-level modulation technique

The $V_\beta$ signal is modulated through the Phase Shifted - Pulse Width Modulation technique (PS - PWM). This modulation technique is like unipolar modulation and so uses the $V_\beta$ signal as input and a second signal identical to the previous one but with a phase shift of 180° between the two signals. The 7-level voltage generation at the inverter's output is achieved through the displacement of the carrier signals by an angle $\phi$ calculated through (5).

$$\phi = 180°/N_{cell} \tag{5}$$

The value of $N_{cell}$ is the number of cells used for the multilevel inverter; in this application, $N_{cell} = 3$ to synthesize the outputs of a 7-level inverter. Each cell uses four control signals which can be seen in the general scheme in Fig. 5 as $PWM\ nx$, where $n$ represents the transistor to be controlled and $x$ the cell to which it belongs. In total, the proposed 7-level inverter needs to generate 12 outputs. This multilevel modulation technique is selected to control each power cell using the same control signal independently and for the multiplicative effect of the modulator output frequency, which allows a low level of harmonic distortion at the output [15]. For this application, a switching frequency of 6 kHz is used, which allows the use of digital controllers with low computational power that require more time to execute the control algorithm.

## IV. SIMULATED RESULTS

The 7-level inverter, including its proposed control algorithm was programmed using Matlab Simulink software to validate the results of the proposed control. The proposed control scheme and the single-phase 7-level inverter that have been studied in this experiment are shown in Fig. 1 and Fig. 2.

### *A. First test*

This experiment is performed with variable solar radiation and no current phase shift to observe the performance of the proposed control during the tracking of the maximum power point while maintaining a purely active power generation. The value of the reference $I_q^*$ is set to zero, and the $I_d^*$ component is equal to the value of the maximum power total current $I_{total}$.

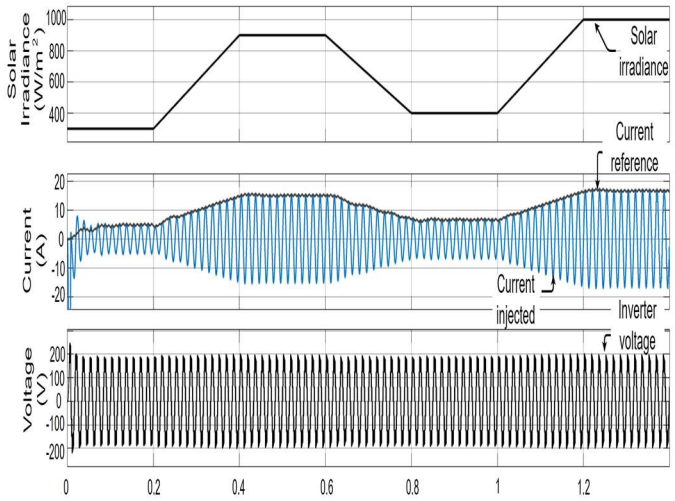

Fig. 6. Performance of the proposed control during peak current tracking with variable solar radiation.

It starts at $t = 0$ with a radiation value of $300\ W/m^2$; this value is maintained until $t = 0.2$ seconds, where an increase reaches $900\ W/m^2$ at $t = 0.4$ seconds.

In Fig. 6, it can be seen how the presented control algorithm can adjust the output current depending on the solar radiation.

At time $t = 0.6$ seconds, solar radiation starts to decrease, and $400\ W/m^2$ is reached at $t = 0.8$ seconds. At time $t = 1$ second, the solar radiation starts a new change, and it reaches $1000\ W/m^2$ at $t = 1.2$ seconds; this value does not change at the end of the simulation at $t = 1.4$ seconds.

During solar radiation changes, the control tries to estimate the current at the point of maximum power through the MPPT algorithms. By locating this value, the maximum power generated by each array of solar panels can be extracted.

The control's efficiency is increased since all the energy produced by the solar panels is used. The efficiency $\eta$ of the proposed control is calculated by (6) using the true power $P_{true}$ and the ideal power $P_{ideal}$ generated by the solar panels.

$$\eta = \frac{P_{true}}{P_{ideal}} \tag{6}$$

$P_{true}$ is calculated through (7) using the voltage and current measurements $I_{p1,2,3}$ and $V_{p1,2,3}$ of each of the three solar panel arrays. This value represents the power generated by each solar panel array used for the multilevel inverter.

$$P_{true} = (I_{p1} * V_{p1}) + (I_{p2} * V_{p2}) + (I_{p3} * V_{p3}) \tag{7}$$

$P_{ideal}$ is estimated at a fixed temperature using (8) and represents the power that the solar panel can ideally generate at a given solar radiation value.

The way to calculate $P_{ideal}$ is through the solar radiation $I_{rr}$ received by the panels, the power delivered by the solar panel, which the manufacturer gives in $W/m^2$, and the number $n$ of solar panels used in the design.

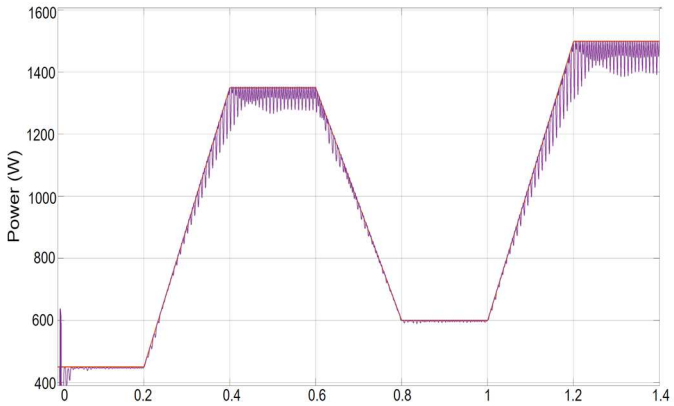

Fig. 7. Ideal power generated by the PV array and true power extracted for the multilevel inverter

$$P_{ideal} = n * I_{rr} * W/m^2 \tag{8}$$

The maximum efficiency calculated through (6), (7), and (8) is 0.99, and a minimum value is 0.96. During the simulation, the efficiency varies inside this range depending on the solar radiation received by the solar panels. In Fig. 7, a graph with the ideal power generated by the solar panels and the true power used for the multilevel inverter can be seen. The ripple in the true power curve generated by the multilevel inverter is due to the charging and discharging of the capacitors connected between each H-bridge and the solar panels. The larger the value of each capacitor, the smaller the ripple in the extracted power. However, a higher value of the capacitors impacts the dynamic response of the proposed control causing it to be slower and insensitive to small changes in solar radiation.

In Fig. 8, it is possible to see a close-up of Fig. 6 showing the instant where the control starts. The control takes three cycles of the grid voltage waveform to begin injecting the current in phase (at $t = 0.04$ seconds) and up to 6 cycles for the peak value of the current waveform to reach the reference value calculated by the MPPT algorithm.

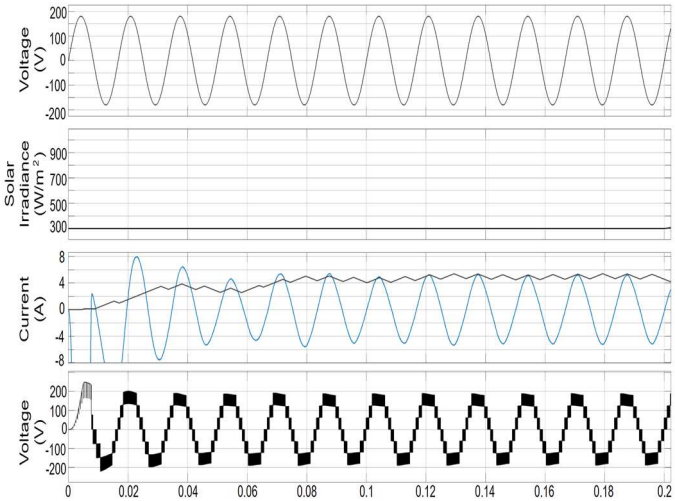

Fig. 8. Time instant at which the proposed control begins to synchronize with the single-phase voltage grid

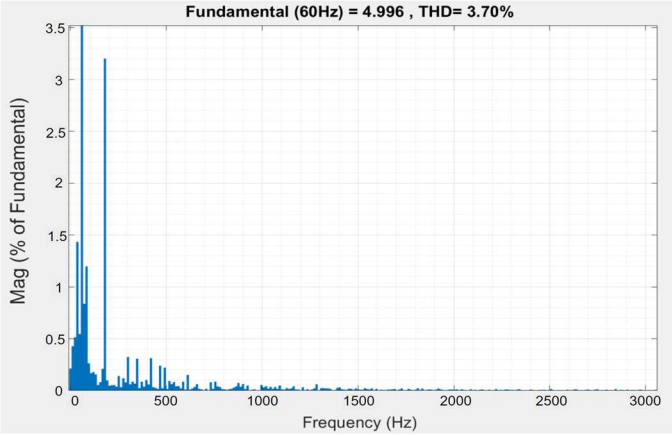


Fig. 9. THD of current with solar radiation of 300 $W/m^2$

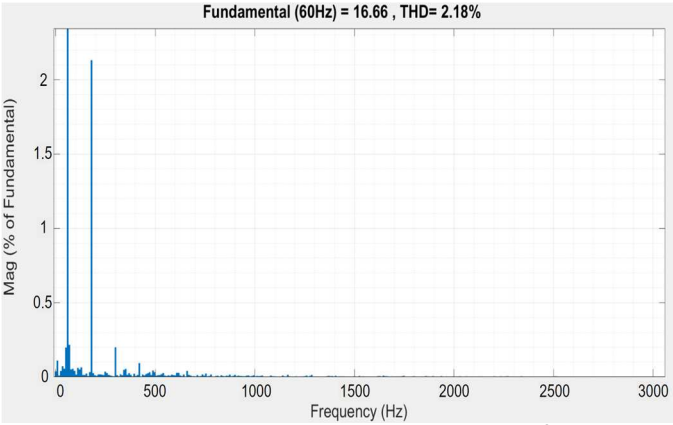


Fig. 10. THD of current with solar radiation of 1000 $W/m^2$

An analysis of the harmonic distortion counting the first 50 harmonics of the current generated by the multilevel inverter is observed in Table II. The THD values are lower than the IEEE Std 519-2014 standard sets as a maximum limit of 5 % in harmonic distortion in the current [16] despite the variable solar radiation. Fig. 9 and Fig. 10 show two of the THD analysis of the current at different solar radiation conditions.

TABLE II THD OF CURRENT

| Solar radiation | THD of current |
|---|---|
| **300 $W/m^2$** | 3.70 % |
| **400 $W/m^2$** | 2.98 % |
| **900 $W/m^2$** | 2.19 % |
| **1000 $W/m^2$** | 2.18 % |

## *B. Second test*

The second experiment allows observing the system's performance when injecting reactive power to the grid through the current phase shift.

For this experiment, constant solar radiation of 700 $W/m^2$ is used and, only the value of the reference currents $I_d^*$ and $I_q^*$ in the PI controls are changed. The experiment starts with 100 % of $I_{total}$ sets in the $I_d^*$ component and 0 % in the $I_q^*$ component.

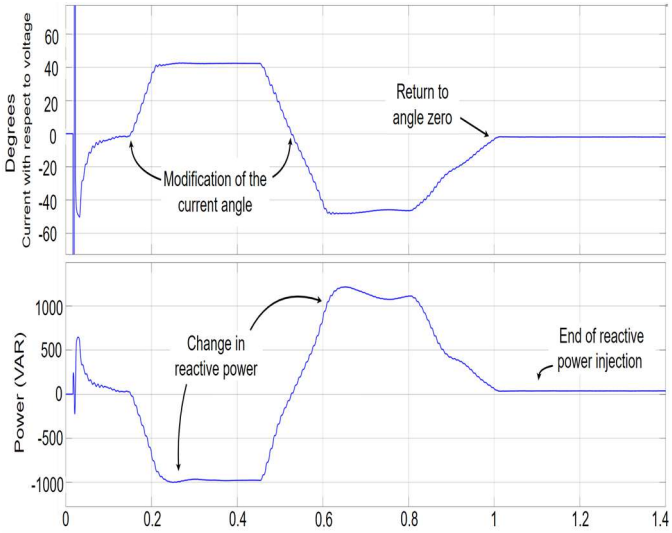


Fig. 11. The angle of the current concerning the voltage and reactive power injected into the grid

At instant $t = 0.142$ second, 70 % of $I_{total}$ is set as the value of $I_q^*$, and the rest is placed in $I_d^*$. It is possible to observe how the reactive power reaches a value of approximately -975 VAR. At this moment, the current overtakes the voltage, and there is an angle between them of 42.5°.

In $t = 0.45$ seconds, a new change in $Iq^*$ is made, and -70% of $I_{total}$ is reached as a new value of $Iq^*$ at $t = 0.6$ seconds. This negative percentage generates a current 47° delayed concerning the grid voltage, and the multilevel inverter generates a reactive power of 1150 VAR.

The time instant where the current and voltage of the multilevel inverter are in phase occurs after time $t = 1$ second. The changes in angle and reactive power injected into the grid can be seen in Fig. 11.

Performing an analysis of the harmonic distortion in the current generated by the 7-level inverter, Table III shows the current THD values during each phase change with constant radiation of 700 $W/m^2$. Fig. 12 and Fig. 13 show the THD analysis of the current when injecting reactive power to the grid.

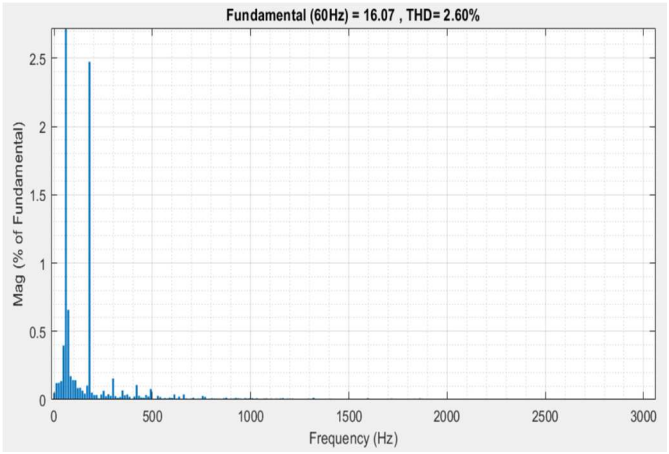


Fig.12. THD of the injected current when generating -975 VAR of reactive power

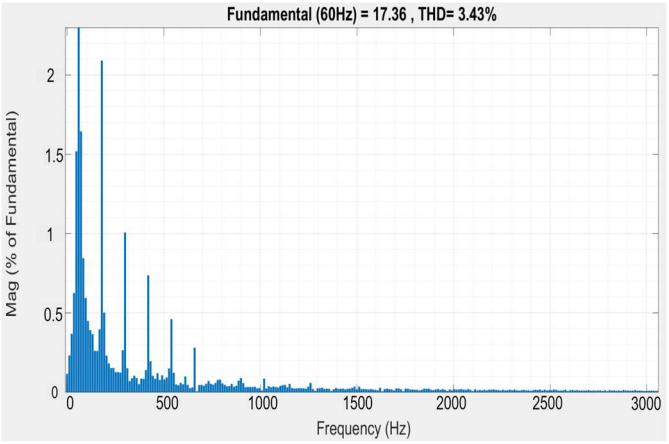

Fig.13. THD of the injected current when generating 1150 VAR of reactive power

TABLE III THD AND REACTIVE POWER GENERATED

| % of $I_d^*$ | % of $I_q^*$ | Reactive power | Angle of the current concerning voltage | THD |
|---|---|---|---|---|
| 30 | +70 | -975 VAR | 42.5° | 2.60 % |
| 30 | -70% | 1150 VAR | -47.0° | 3.43 % |

## V. CONCLUSIONS

In this paper, a new simplified control technique based on d-q theory is proposed for photovoltaic power generation using a monophasic single-stage 7-level inverter. The hardware topology employed allows fewer power components, thus increasing the system's efficiency compared to two-stage 7-level inverters. Furthermore, the control allows the injection of alternating current in phase with the grid or with a phase shift that the user can adjust. As a result, the current generated by the inverter has a THD lower than stipulated by IEEE Std 519-2014 with changing solar radiation without current phase shift or with constant solar radiation but with varying current-phase.
The proposed control does not have a solar radiation balancing stage, requiring fewer computational processes, and favors its implementation on digital processing systems with low computational power.

## REFERENCES

[1] A. Sarkar, S. Reddy, B. Das, P. R. Kasari, A. Saha, and A. Chakrabarti, "Multilevel inverter based single stage grid connected solar PV," Proc. 2015 Int. Conf. Green Comput. Internet Things, ICGCIoT 2015, no. 4, pp. 1217–1222, 2016, doi: 10.1109/ICGCIoT.2015.7380649.

[2] R. Khawaja, F. Sebaaly, and H. Y. Kanaan, "Design of a 7-Level Single-Stage/Phase PUC Grid-Connected PV Inverter with FS-MPC Control," Proc. IEEE Int. Conf. Ind. Technol., vol. 2020-Febru, pp. 751–756, 2020, doi: 10.1109/ICIT45562.2020.9067338.

[3] W. Sripipat and S. Po-Ngam, "Simplified active power and reactive power control with MPPT for single-phase grid-connected photovoltaic inverters," 2014 11th Int. Conf. Electr. Eng. Comput. Telecommun. Inf. Technol. ECTI-CON 2014, pp. 4–7, 2014, doi: 10.1109/ECTICon.2014.6839805.

[4] M. Reveles-Miranda, M. Flota-Banuelos, F. Chan-Puc, V. Ramirez-Rivera, and D. Pacheco-Catalan, "A Hybrid Control Technique for Harmonic Elimination, Power Factor Correction, and Night Operation of a Grid-Connected PV Inverter," IEEE J. Photovoltaics, vol. 10, no. 2, pp. 664–675, Mar. 2020, doi: 10.1109/JPHOTOV.2019.2961600.

[5] M. Morales-Caporal, J. Rangel-Magdaleno, H. Peregrina-Barreto, and R. Morales-Caporal, "FPGA-in-the-loop simulation of a grid-connected photovoltaic system by using a predictive control," Electr. Eng., vol. 100, no. 3, pp. 1327–1337, Sep. 2018, doi: 10.1007/s00202-017-0596-1.

[6] Solartec, "SOLARTEC | Paneles Solares," Solartec, Aug. 24, 2014. http://i3g.mx/panel/prod_s60mc.html (accessed Jun. 23, 2021).

[7] M. Morales-Caporal, J. Rangel-Magdaleno, and R. Morales-Caporal, "Digital simulation of a predictive current control for photovoltaic system based on the MPPT strategy," in International Power Electronics Congress - CIEP, Aug. 2016, vol. 2016-August, pp. 295–299, doi: 10.1109/CIEP.2016.7530773.

[8] S. Mishra and A. N. Tiwari, "Simulation and Analysis of Open Loop PV system with Double Stage Conversion," 2020 Int. Conf. Comput. Perform. Eval. ComPE 2020, pp. 491–496, 2020, doi: 10.1109/ComPE49325.2020.9200104.

[9] Y. Wang and X. Yu, "Comparison study of MPPT control strategies for double-stage PV grid-connected inverter," IECON Proc. (Industrial Electron. Conf., pp. 1561–1565, 2013, doi: 10.1109/IECON.2013.6699365.

[10] B. Crowhurst, E. F. El-Saadany, L. El Chaar, and L. A. Lamont, "Single-phase grid-tie inverter control using DQ transform for active and reactive load power compensation," PECon2010 - 2010 IEEE Int. Conf. Power Energy, pp. 489–494, 2010, doi: 10.1109/PECON.2010.5697632.

[11] Wurth Elektronik, "Advantages and Disadvantages of Common Mode Chokes," Wurth Elektronik, Mar. 18, 2016. https://www.we-online.com/web/en/electronic_components/news_pbs/blog_pbcm/blog_detail-worldofelectronics_61438.php (accessed Jun. 23, 2021).

[12] S. Jain and V. Agarwal, "Comparison of the performance of maximum power point tracking schemes applied to single-stage grid-connected photovoltaic systems," IET Electr. Power Appl., vol. 1, no. 5, pp. 753–762, 2007, doi: 10.1049/iet-epa.

[13] A. DOLARA, R. FARANDA, and S. LEVA, "Energy Comparison of Seven MPPT Techniques for PV Systems," J. Electromagn. Anal. Appl., vol. 01, no. 03, pp. 152–162, 2009, doi: 10.4236/jemaa.2009.13024.

[14] M. A. Morales Caporal, J. D. J. Rangel Magdaleno, I. Cruz Vega, and R. Morales Caporal, "Improved grid-photovoltaic system based on variable-step MPPT, predictive control, and active/reactive control," IEEE Lat. Am. Trans., vol. 15, no. 11, pp. 2064–2070, 2017, doi: 10.1109/TLA.2017.8070409.

[15] J. Rodriguez et al., "Multilevel Converters: An Enabling Technology for High-Power Applications," Proc. IEEE, vol. 97, no. 11, pp. 1786–1817, Nov. 2009, doi: 10.1109/JPROC.2009.2030235.

[16] IEEE Power and Energy Society, "IEEE Recommended Practice and Requirements for Harmonic Control in Electric Power Systems IEEE Power and Energy Society," vol. 2014, 2014, doi: 10.1109/IEEESTD.2014.6826459.